

The effects of Bone Remodeling on Biomechanical Behavior in a Patient with an Implant-Supported Overdenture

Sato, Emika; Shigemitsu, Ryuji; Mito, Takehiko; Yoda, Nobuhiro; Rasmussen, John; Sasaki, Keiichi

Published in:
Computers in Biology and Medicine

DOI (link to publication from Publisher):
[10.1016/j.compbiomed.2020.104173](https://doi.org/10.1016/j.compbiomed.2020.104173)

Creative Commons License
CC BY-NC-ND 4.0

Publication date:
2021

Document Version
Publisher's PDF, also known as Version of record

[Link to publication from Aalborg University](#)

Citation for published version (APA):

Sato, E., Shigemitsu, R., Mito, T., Yoda, N., Rasmussen, J., & Sasaki, K. (2021). The effects of Bone Remodeling on Biomechanical Behavior in a Patient with an Implant-Supported Overdenture. *Computers in Biology and Medicine*, 129, Article 104173. <https://doi.org/10.1016/j.compbiomed.2020.104173>

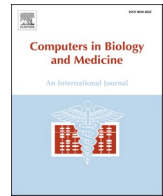
General rights

Copyright and moral rights for the publications made accessible in the public portal are retained by the authors and/or other copyright owners and it is a condition of accessing publications that users recognise and abide by the legal requirements associated with these rights.

- Users may download and print one copy of any publication from the public portal for the purpose of private study or research.
- You may not further distribute the material or use it for any profit-making activity or commercial gain
- You may freely distribute the URL identifying the publication in the public portal -

Take down policy

If you believe that this document breaches copyright please contact us at vbn@aub.aau.dk providing details, and we will remove access to the work immediately and investigate your claim.



The effects of bone remodeling on biomechanical behavior in a patient with an implant-supported overdenture

Emika Sato^a, Ryuji Shigemitsu^{a,b,*}, Takehiko Mito^a, Nobuhiro Yoda^a, John Rasmussen^b, Keiichi Sasaki^a

^a Division of Advanced Prosthetic Dentistry, Tohoku University Graduate School of Dentistry, Sendai, 980-8575, Japan

^b Department of Materials and Production, Aalborg University, Fibigerstrade 16, Aalborg East, DK, 9220, Denmark

ARTICLE INFO

Keywords:

Dental implant
Overdenture
Finite element analysis
Mechanical stimulus
Bone remodeling

ABSTRACT

This study aimed to clarify the effects of bone remodeling on biomechanical behavior in a patient with a mandibular implant-supported overdenture by comparing computed tomography-based finite element analyses (CT-FEA) with two time points of CT data. The present FEA was based on CT data collected from a 62-year-old female subject, who wore a mandibular implant overdenture supported by four dental implants with bar attachment. Two kinds of FE models were constructed from CT data taken at two time points: pre-implantation (Original-model) and 12 years post-implantation (Aged-model). FE models consisted of patient-specific model geometry and heterogeneous material properties. The deviation analysis was carried out to assess the changes in bone mass over a period of 12 years. The results show an averaging of intraosseous stress and strain energy density between the implant regions in the Aged-model. The results of the morphological assessments demonstrated that the bone mass and quality had significantly changed over 12 years. Area-specific bone resorption was also observed at the bone surrounding each implant. The combined findings indicate that the averaging of mechanical variables was due to chronological changes in bone morphology, suggesting adaptation to mechanical loads by peri-implant bone remodeling.

1. Introduction

Long-term clinical complications of dental implant treatment processes are typically peri-implantitis and peri-implant mucositis, which are inflammation in peri-implant tissues caused by bacterial infections [1–3]. On the other hand, a large number of mechanical complications such as fractures and loosening of implant component have also been reported [4,5]. Those mechanical complications are considered to be results of functional processes; occlusal forces occurring from mastication and/or bruxism are transmitted to implant prostheses, causing stresses and strains in the components, resulting in the aforementioned complications. In addition, it is reported that the mechanical stress and strain developed in the peri-implant bone plays an essential role in maintaining homeostasis of the bone [6,7]. Thus, it is necessary to control the biomechanical conditions in implant components and bone for the long-term prognosis of dental implants as well as avoiding infections in tissues surrounding implants.

The biomechanical studies related to dental implant treatment and

prosthodontic treatment have been based on *in-vitro* mechanical testing such as single load to failure [8], fatigue testing [9], physical model experiments [10–12], digital image correlation [13], *in vivo* biomechanical testing with strain gauges [14] and pressure-sensitive sheets [15,16], and computer simulations with finite element analysis (FEA) [17]. FEA has developed from simple models to nonlinear analysis considering dynamic loading conditions and nonlinear characteristics of materials, due to the improvement of computer-aided engineering [18–21]. Recent FEA studies of dental implants have used complicated shape models constructed from CT data as well as nonlinear analysis models considering friction between implant components [22,23]. However, few studies perform longitudinal simulations rely on subject-specific data of individual patient [24].

A previous study [25] has successfully measured actual loads exerted on a tooth during function in the oral cavity of a subject using a 3-D piezo-electric force transducer. Yoda et al. [26] applied the measuring system for an implant-supported prosthesis to measure the loads in the implant abutments. In addition, Shigemitsu et al. [27] clarified the

* Corresponding author. Division of Advanced Prosthetic Dentistry, Tohoku University Graduate School of Dentistry, Sendai, 980-8575, Japan.

E-mail address: ryuji.shigemitsu.d7@tohoku.ac.jp (R. Shigemitsu).

<https://doi.org/10.1016/j.complbiomed.2020.104173>

Received 6 December 2020; Received in revised form 9 December 2020; Accepted 9 December 2020

Available online 13 December 2020

0010-4825/© 2020 The Authors.

Published by Elsevier Ltd.

This is an open access article under the CC BY-NC-ND license

(<http://creativecommons.org/licenses/by-nc-nd/4.0/>).

effects of the number and direction of installed implants on intraosseous stresses by means of personalized FE models based on CT data and intraorally measured loads as loading conditions. However, such models represented snapshots in time and could not involve temporal changes of jaw bone.

The aim of this study was to clarify the biomechanical behavior related to temporal morphological changes in a patient with an implant-supported overdenture by comparing personalized finite element analyses based on CT data of the patient between two time points: FE models constructed from CT data taken before dental implant placement and 12 years post-implantation.

2. Materials and methods

This study was approved by the Ethics Committee of Tohoku University Graduate School of Dentistry and conducted with the informed consent related to the purpose of this study and management of personal information.

The subject was a female patient aged 62 with a complete denture on her edentulous maxilla. The four implant fixtures (Mk III TiU RP, Nobel Biocare, Japan) with a diameter of 3.75 mm and a length of 13 mm were placed in the mandibular bone between the bilateral mental foramina. The four implants supported a complete overdenture with a bar attachment. The implant fixtures were splinted with the bar attachment and connected to each abutment with a titanium screw (Fig. 1).

2.1. In-vivo load measurements and loading conditions

The four implants were defined as Imp 1, Imp 2, Imp 3, and Imp 4 from the right (Fig. 1a). The three-dimensional intraoral load measurement during maximal voluntary clenching (MVC) was performed using 3-D piezo-electric force transducers (Type Z18400, Kistler Instrument, Japan) [26]. The transducers were fixed to implant fixtures with custom-made jigs (Fig. 1a). The measurement protocol is detailed in a previous study [27]. The load vector during MVC measured by the transducer on each implant was transformed to the coordinate with vertical (z), antero-posterior (y) and mediolateral (x) axes based on the mandibular plane and sagittal plane (Table 1).

2.2. FE modeling

Two FE models based on the subject's CT data were constructed. The first model, Model A (Original model), was based on the CT data (Quantex, GE Yokogawa Medical Systems, Tokyo, Japan) taken at the pre-surgery initial consultation. In the interest of minimization of radiation and absence of medical indication, CT data could not be taken at post-surgery. Therefore, Model A was constructed by *in-silico* placement of the implants. The position of each implant to the mandibular bone

Table 1

In vivo measured loads during MVC.

	Loading vector(N)			
	F(x)	F(y)	F(z)	F
Imp1	-11.4	10.7	-41.1	44.0
Imp2	3.2	-11.0	-39.8	41.5
Imp3	11.1	-12.1	-40.3	43.5
Imp4	33.2	0.1	-54.5	63.8

was determined by cephalometric analyses described in detail in a previous study [27]. CT data (Aquilion ONE, Toshiba Corporation Medical Systems, Tokyo, Japan) for the second model, Model B (Aged Model), were collected at the age of 74, 12 years post-implantation. To reduce the beam hardening and metal artifacts, the CT data were reconstructed using single-energy metal artifact reduction algorithm (SEMAR) supplied with the CT examination system [28,29]. In this technique, the metal images were segmented on the original images and used to correct the raw data. Classification of various tissues is subsequently performed. These information were combined with the original raw data iteratively to reduce the beam hardening and metal artifacts (Fig. 2). The reconstructed data were finally combined and used in the segmentation process of FE modeling. Both CT scan images were obtained with a matrix of 512×512 , a field of view of 160 mm, tube voltage 125 kV, and a slice thickness of 0.5 mm. FEA software (MECHANICAL FINDER Ver. 7.0 Extended Edition, Research Center for Computational Mechanics, Tokyo, Japan) was used to create two FE models. The geometries of implant components, including fixtures, measuring devices and a connecting bar of attachment, were recorded using a micro focus X-ray apparatus and reconstructed in the model.

In both models, perfect adhesion between the implants and the surrounding bone was assumed, simulating osseointegration. In Model A, area behind the bilateral mandibular ramuses were completely constrained. In Model B, bilateral mandibular condyles were completely constrained (Fig. 3).

The loads were applied to each implant where the load measuring devices were mounted (Fig. 3). Magnitude and direction of loads applied on the individual implants were the maximum values of the loads on the respective implants, measured in the subject during her MVC (Table 1).

The 4-node tetrahedral elements with edge length of 0.25–1.0 mm and an aspect ratio ranging from 1.0 to 19.8 were employed for modeling. The outer surface of the cortical bone was modelled with 3-node shell elements for the purpose of minimizing the impact of the partial volume effect [30]. A convergence test with mesh refinements was performed to verify the model quality using the average of von Mises stress in the mandibular bone with a convergence criterion of 3%, i.e. the model was considered converged upon a change below 3% in the final refinement step (Fig. 4). Based on the results of the convergence

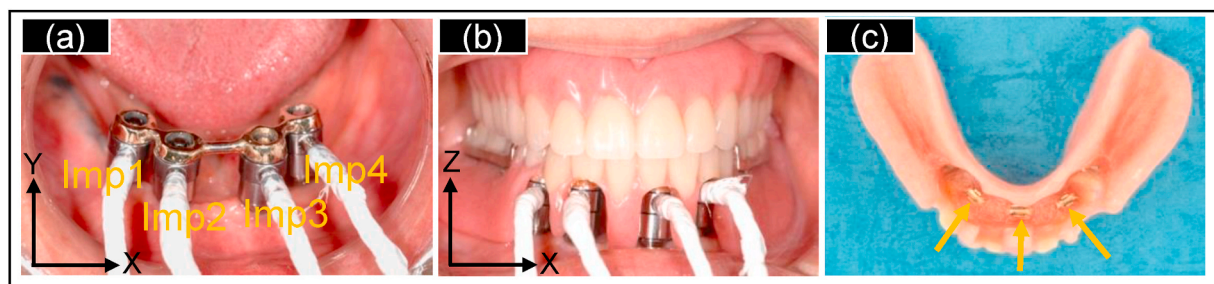


Fig. 1. The subject had a maxillary full denture and a bar-and-clip overdenture supported by four dental implants that were placed into the mandibular bone. The coordinate system was defined as vertical (z), antero-posterior (y) and mediolateral (x) axes based on the mandibular plane and sagittal plane. (a) The load-measuring device in the mouth (b) *in vivo* loads during maximum voluntary clenching were recorded (c) The overdenture had 3 clip attachments that were connected with bar splinting 4 implants during function.

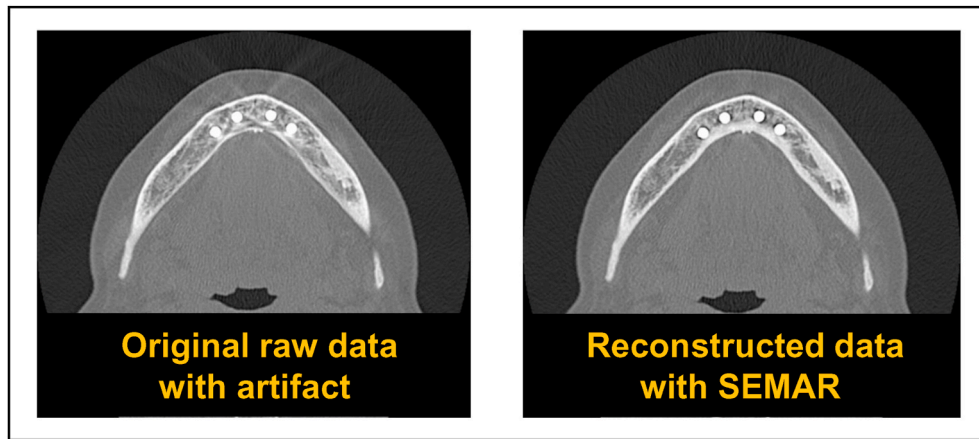


Fig. 2. In this algorithm, classification of tissues was conducted iteratively to reduce the beam hardening and metal artifacts.

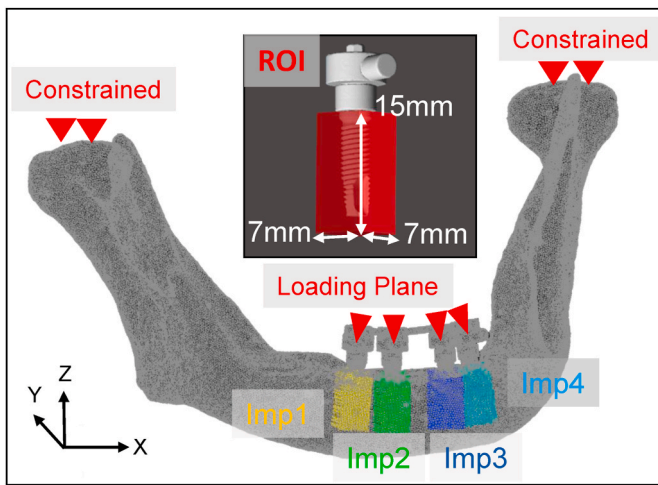


Fig. 3. In Model B, bilateral mandibular condyles were completely constrained. The loads were applied to each implant where the load measuring devices were mounted. In both models, region-of-interest (ROI) was defined as box volumes with dimensions 7 mm by 7 mm by 15 mm surrounding each implant.

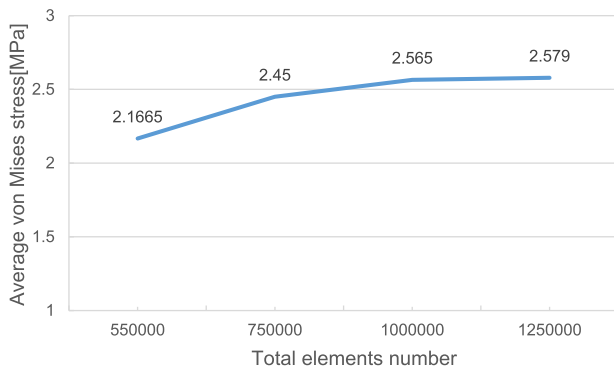


Fig. 4. A convergence test with mesh refinements was performed to verify the model quality using the average of von Mises stress in the mandibular bone. Based on the results of the convergence testing, the mesh size and numbers were decided in each model.

testing, the models comprised 1,278,059 elements and 241,734 nodes for Model A and 2,740,363 elements and 500,382 nodes for Model B.

The material properties in both models are summarized in Table 2. After defining regions-of-interest of the bone area, the material

heterogeneity of the inside of the mandibular bone was reproduced in each model. The volumetric bone mineral density (ρ) was calculated from the average HU value for each element by previously published equations [31,32]. The two CT in this study were taken with the same energy level and, thus, the HU-BMD relationships were assumed to be the same despite differences in CT equipment.

$$\rho(\text{g/cm}^3) = [\text{H.U.} + 1.4246] \times 0.001/1.058 \quad (\text{HU} > -1) \quad (1)$$

$$\rho(\text{g/cm}^3) = 0 \quad (\text{HU} \leq -1) \quad (2)$$

The elastic modulus (MPa) corresponding to the volumetric bone density in each element was calculated using the following equation [33].

$$E \text{ (MPa)} = 0.001 [\rho = 0] \quad (3)$$

$$E \text{ (MPa)} = 33,900\rho^{2.20} \quad [0 < \rho \leq 0.27] \quad (4)$$

$$E \text{ (MPa)} = 5,307\rho + 469[0.27 < \rho < 0.6] \quad (5)$$

$$E \text{ (MPa)} = 10,200\rho^{2.01}[\rho \geq 0.6] \quad (6)$$

Poisson's ratio was set as 0.4 for both cortical and cancellous bone [33].

Isotropic and homogeneous material properties were assumed for the implant components and connecting bar which were determined from a previous study [27].

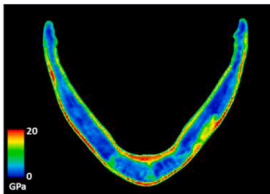
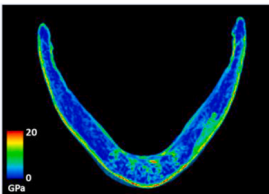
2.3. FE analysis

The von Mises equivalent stress (VMS), the maximum principal stress (Sigma1), minimum principal stress (Sigma3) and strain energy density (SED) were computed to observe mechanical stimulus in both models. In both models, region-of-interest (ROI) was defined as box volumes with dimensions 7 mm by 7 mm by 15 mm surrounding each implant (Fig. 3). Volume average values for VMS, Sigma1, Sigma3 and SED in the ROI were calculated. Weighted histograms (weighted by element volume) with 100 bins for SED of elements in the ROI were used to compare the mechanical state around four implants in each model quantitatively, despite their different element configurations. SED is commonly considered to be a determining factor for bone remodeling [24,34,35].

2.4. Morphological assessments of the mandibular bone

To evaluate morphological changes of the mandibular bone between the two time points, the two models were registered to each other and superimposed by voxel processing software (VOXELCON, Quint

Table 2
The material properties of FE models.

	Original-model (Model-A)		Aged-model (Model-B)	
	Young's modulus (MPa)	Poisson's ratio	Young's modulus (MPa)	Poisson's ratio
Cortical bone and Cancellous bone	Heterogeneous values	0.4	Heterogeneous values	0.4
Implant component and Connecting bar (Pure titanium)	106,000	0.34	106,000	0.34
Distribution of Young's modulus				
CT image	pre-implantation		12 years post-implantation	

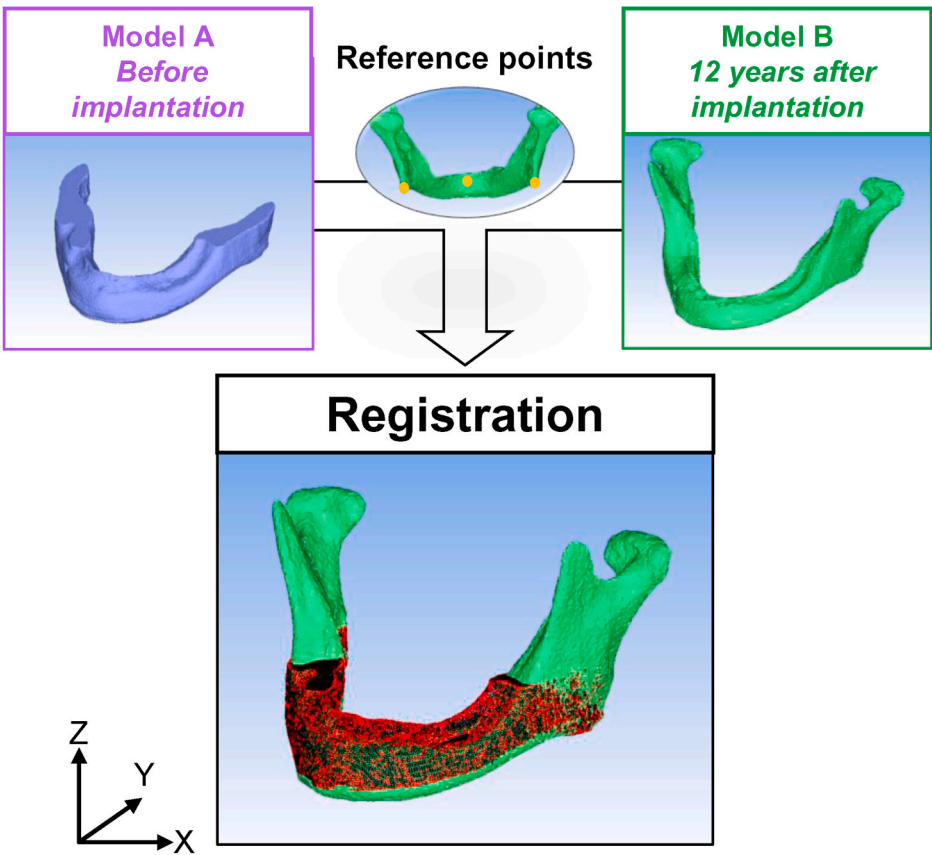


Fig. 5. The series of CT images at two time points-before implants placement and 12 years after placements were converted to the STL data and registered for evaluating morphological changes. Reference points for registration were three points consisting of both angles of the mandible and spina mentalis.

Corporation, Japan). Reference points for registration were three points consisting of the two angles of the mandible and spina mentalis, then vertical dimensional changes were morphologically calculated (Fig. 5).

3. Results

3.1. Results of FE analyses

Fig. 6 shows the distribution of each mechanical stimulus on the mandibular bone surface. In Model A, concentration of VMS, Sigma3 and SED occurred at the distal parts of Imp3 and Imp4, while the stress and strain state around the implants appeared to be more averaged in Model B. Fig. 7 shows the distribution of each mechanical stimulus in a

cross section through the two medial implant holes (Imp2 and Imp3). In a cross-sectional plane, compared to Model A, Model B demonstrated concentrated VMS, Sigma3 and SED areas in the buccal cortical bone and changes in VMS, Sigma1, Sigma3 and SED distribution tendency in the cancellous bone.

Fig. 8 shows volume average values of mechanical stimuli around each implant (ROI) in two models. In Model A, relatively higher VMS were observed at Imp4 compared to the other implant. In Model B, VMS and Sigma1 were more averaged between each implant, possibly caused by changes in the shapes and material properties of the mandibular bone. In contrast, the mechanical state around each implant was not changed for Sigma3 and SED in Model B compared to Model A.

Fig. 9 shows weighted histograms of strain energy densities

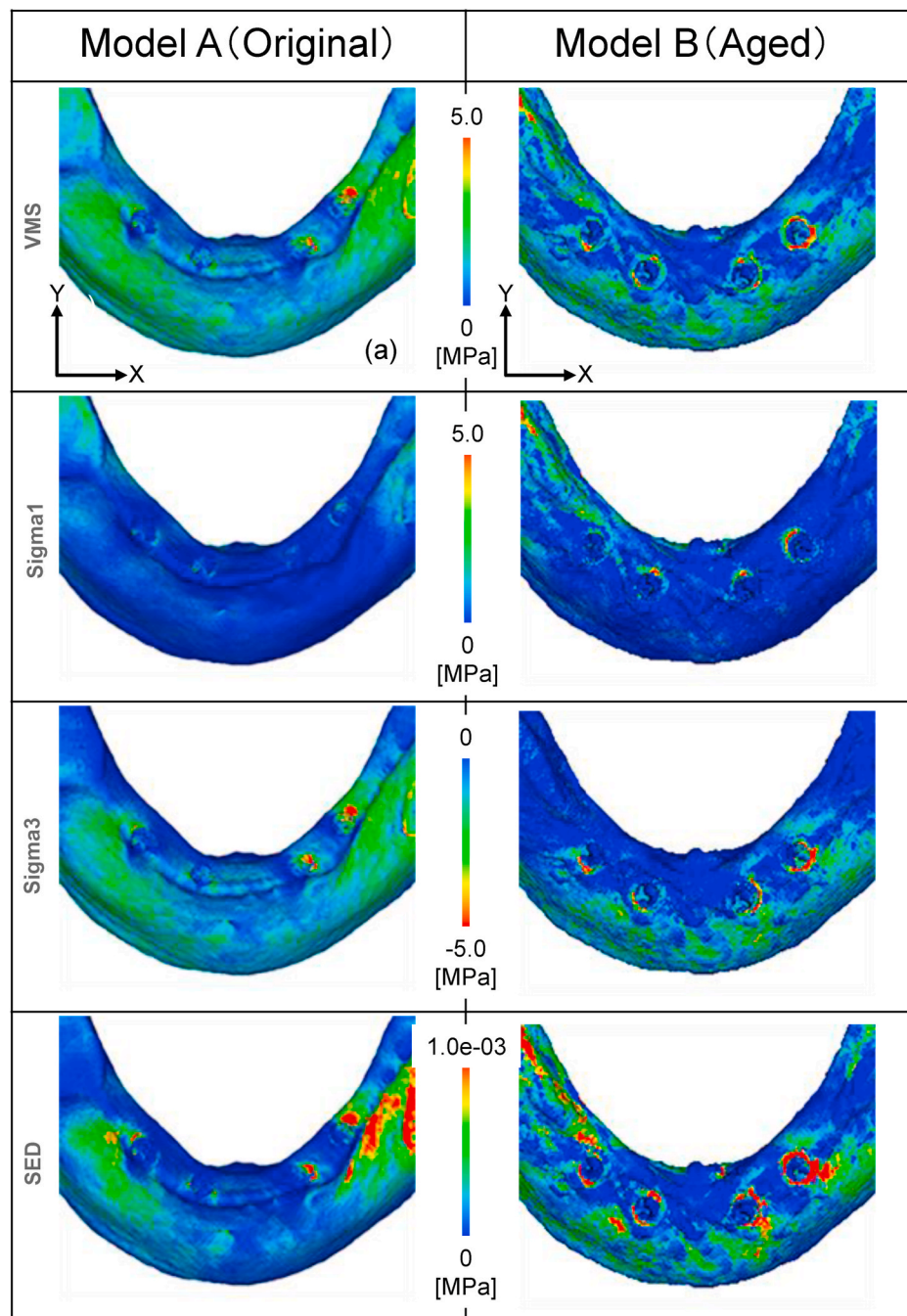


Fig. 6. The distribution of VMS, Sigma1, Sigma3, and SED on the mandibular bone surface and in a cross section. Model A (Original Model: pre-implantation), Model B (Aged Model: 12 years post-implantation).

separated into the regions-of-interest surrounding the four implants in the two models. The SED was generally higher and more averaged between the implants in Model B, i.e. Model B shows a higher degree of load sharing between the implants.

3.2. Results of morphological assessment of the mandibular bone

Fig. 10 shows the morphological differences of the mandibular bone shape between the two time points. Focusing on site-specific resorption, large amounts of bone resorption were observed surrounding Imp1, Imp2 and Imp3 compared to Imp4 (Fig. 10a). In addition, the relative location between each implant and the bone had significantly changed after 12 years of implantation (Fig. 10b).

4. Discussion

In the human body, the shape, density and quality of bone varies from point to point and over time in response to mechanobiological circumstances. This phenomenon is called “Bone Remodeling” [36]. This study focused on the effects of bone remodeling on the stress and strain response of the bone in a patient with an implant-supported overdenture. FEA models for the subject at two time points were constructed from geometry and material properties originating from CT images.

Previous biomechanical studies [21,24,37–39], evaluated the mechanical state through different biomechanical variables. The principal stresses are suited for the observation of tensile and compressive stress,

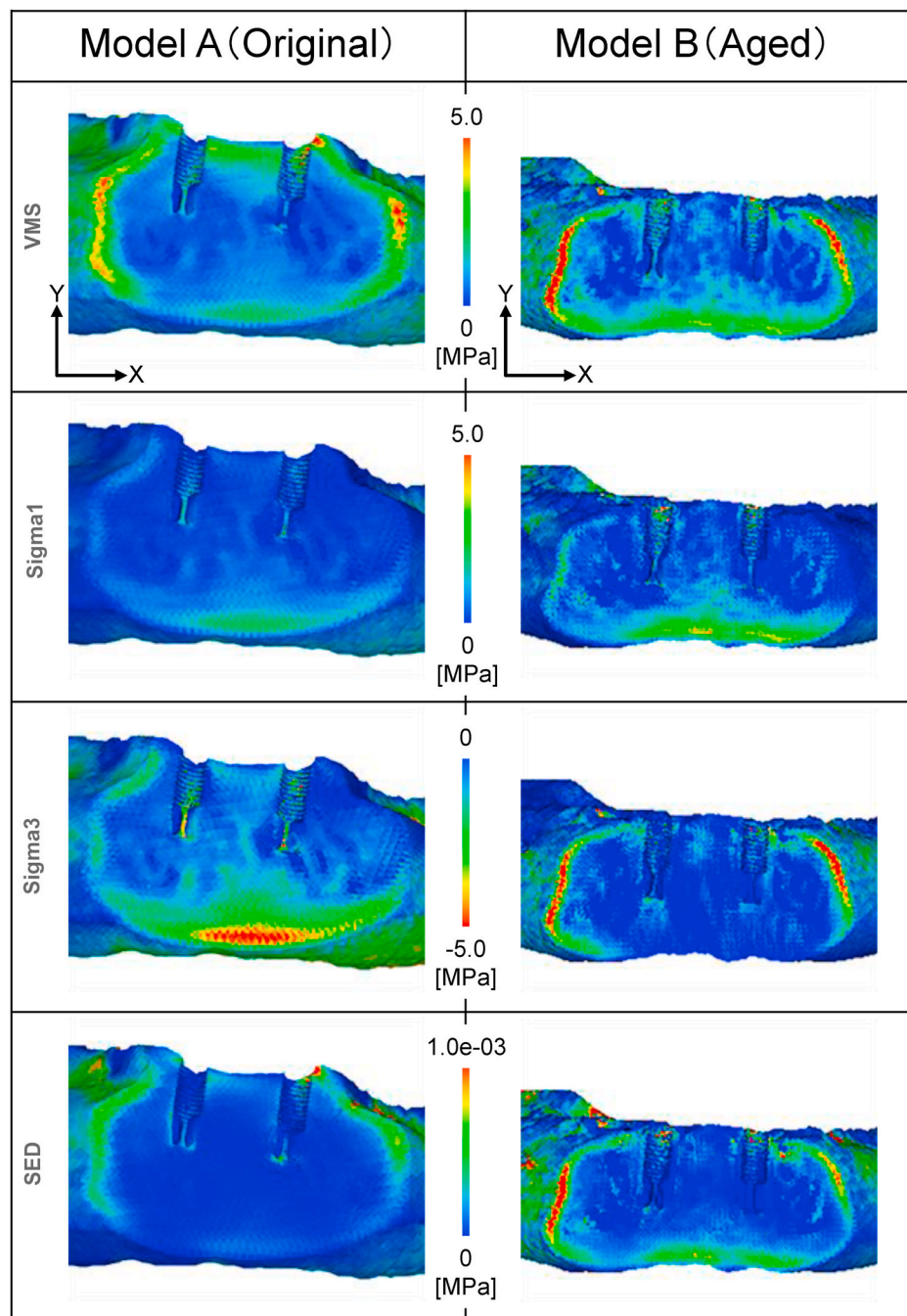


Fig. 7. The distribution of VMS, Sigma1, Sigma3, and SED in the cross section. Model A (Original Model: pre-implantation), Model B (Aged Model: 12 years post-implantation).

whereas the von Mises yield criterion is the most commonly used scalar-valued invariant to evaluate yielding/failure behavior of various materials. Since bone has both elastic and plastic response in physical terms [40,41], the use of the VMS, Sigma1 and Sigma3 can be argued, although bone is hardly a homogeneous material. The SED is also a mechano-biological state variable frequently used in simulation studies focusing on adaptive bone remodeling [35,42,43]. Their investigations were based on the assumption that bone strives to equalize the strain energy per unit of bone mass, averaged over a particular loading history. Besides, Yoda et al. compared relationships between peri-implant bone thickness in actual patients and calculated SED in the bone [24]. Based on these previous studies, the von VMS, Sigma1, Sigma3 and SED were employed to evaluate mechanical behaviors.

In this study, the contour distribution of Model B, developed from CT data of the mandibular bone 12 years post-implantation, demonstrated qualitative redistribution of mechanical stimuli in the cortical bone around the neck of each implant (Fig. 6) and cancellous bone (Fig. 7). Volume average values of VMS and Sigma1 demonstrated quantitative averaging between each implant (Fig. 8). Besides SED-weighted histograms of each implant showed a redistribution of the load between the implants (Fig. 9). These findings may be attributed to physical factors such as differences of geometries and material properties of the bone, and to measurement accuracy differences between the two CT scanners. In support of the physical factors, we notice the moderate to large temporal changes in the morphological assessments of the mandibular bone in terms of bone resorption surrounding Imp1, Imp2, and Imp3

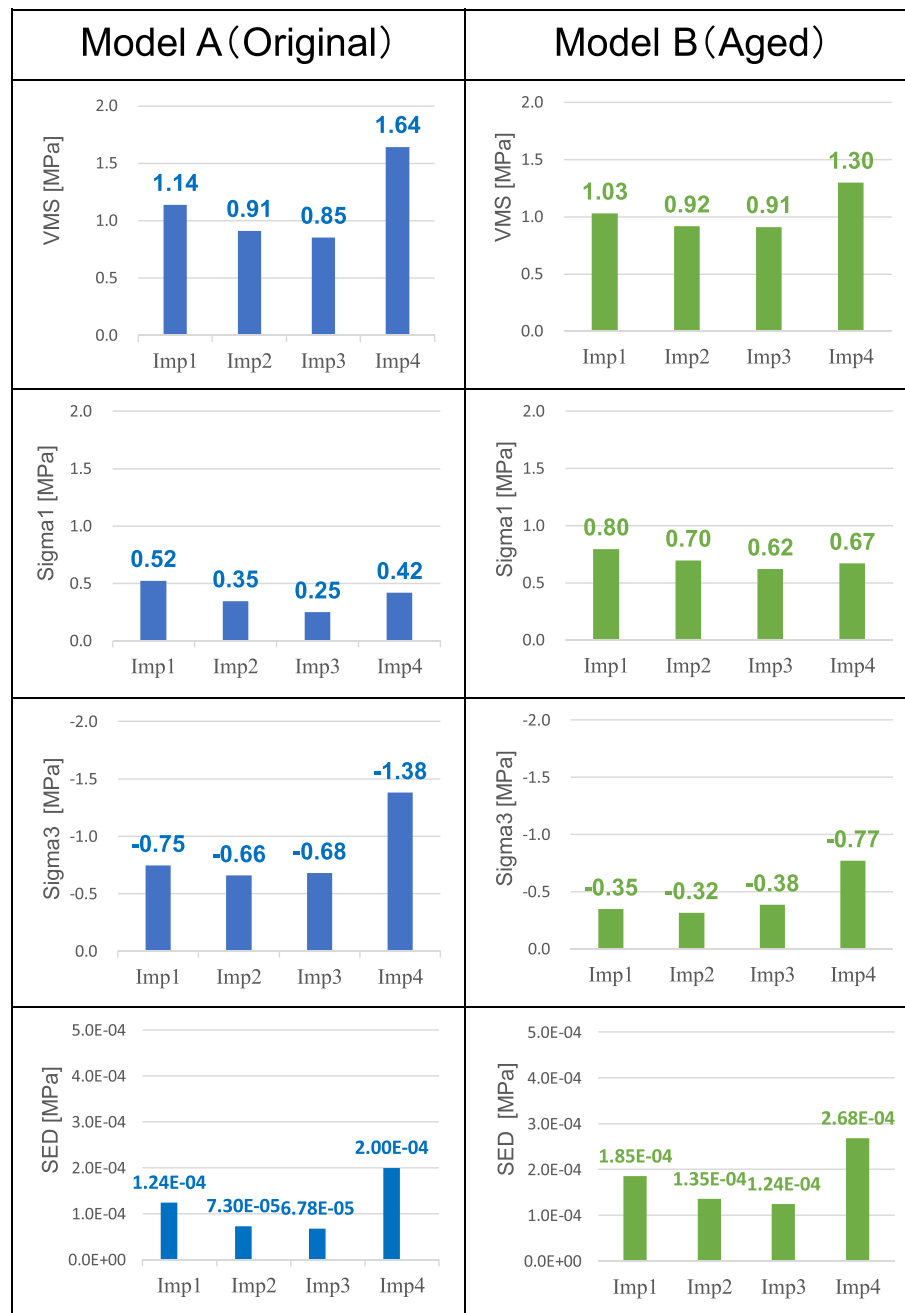


Fig. 8. The volume average values of VMS, Sigma1, Sigma3, and SED at the ROI in Model A and Model B. The ROI was defined as box volumes surrounding each implant.

compared to Imp4 (Fig. 10). These morphological changes caused by bone remodeling correspond with the averaging of the volume average values of VMS and Sigma1 stress around each implant in model B (Fig. 8). Although the mandibular bone shape (residual ridge height) of the subject was originally asymmetric in Model A, which was changed to be mostly horizontally symmetric over the 12 years in Model B (Fig. 10).

Table 2 documents the material properties of the bone at the two time points by Young's modulus distribution. The correlation between residual ridge height, CT values and aging difference were reported in a previous study [44]. The subject in the present study shows large resorption of the height of the residual ridge over 12 years, which might significantly change CT-estimated Young's moduli. However, it should be noted that the equation to calculate Young's moduli is based on the HU-BMD relationship in this study. Even though the two different scans were taken with the same tube voltage, each CT scanner has specific

polychromatic characteristics of the X-ray beam, and other factors might also affect HU. But in this study, we focused on the mechanical state around each implant in each model. Thus, the differences of material properties between Model A and Model B are acceptable.

In summary, the stress and strain fields of the ROI between the individual implants were averaged in Model B compared to in Model A. This is likely due to morphological changes of the bone as a mechano-biological response to the loading and bone metabolic response. Although this study is based on a single subject from which a general trend cannot be derived, the results indicate the dependency of bone remodeling on the mechanical state as observed by Wolff [45]. However, it should be noted that the loading conditions of daily living are different from the idealized loading of the models, and that the same loading conditions were used in Models A and B whereas they may change over time.

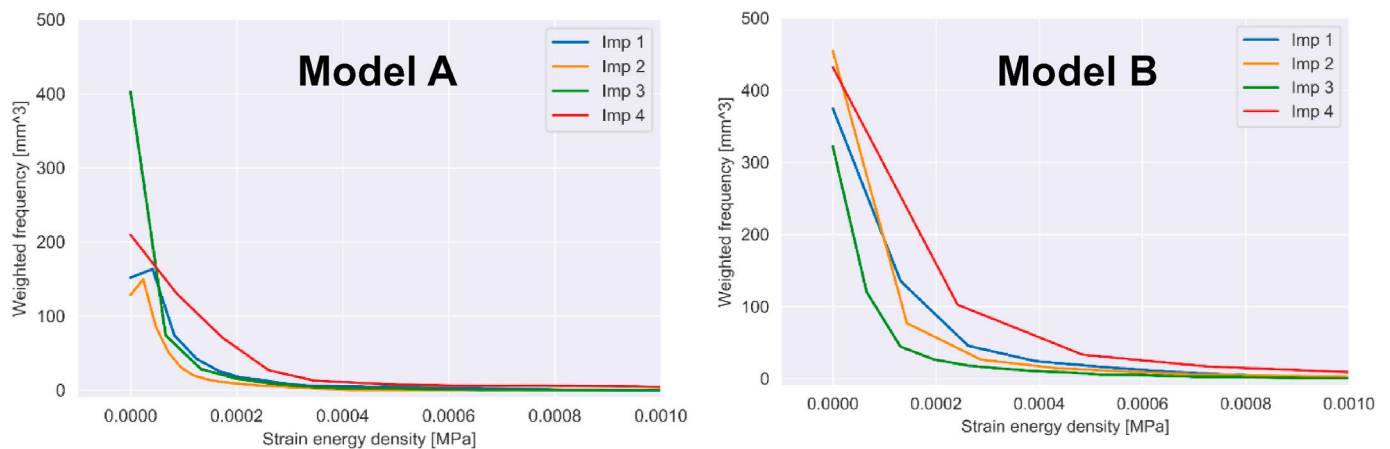


Fig. 9. The weighted histograms (weighted by element volume) with 100 bins for strain energy density of elements in the regions-of-interest were used to compare the models quantitatively despite their different geometries and element configurations.

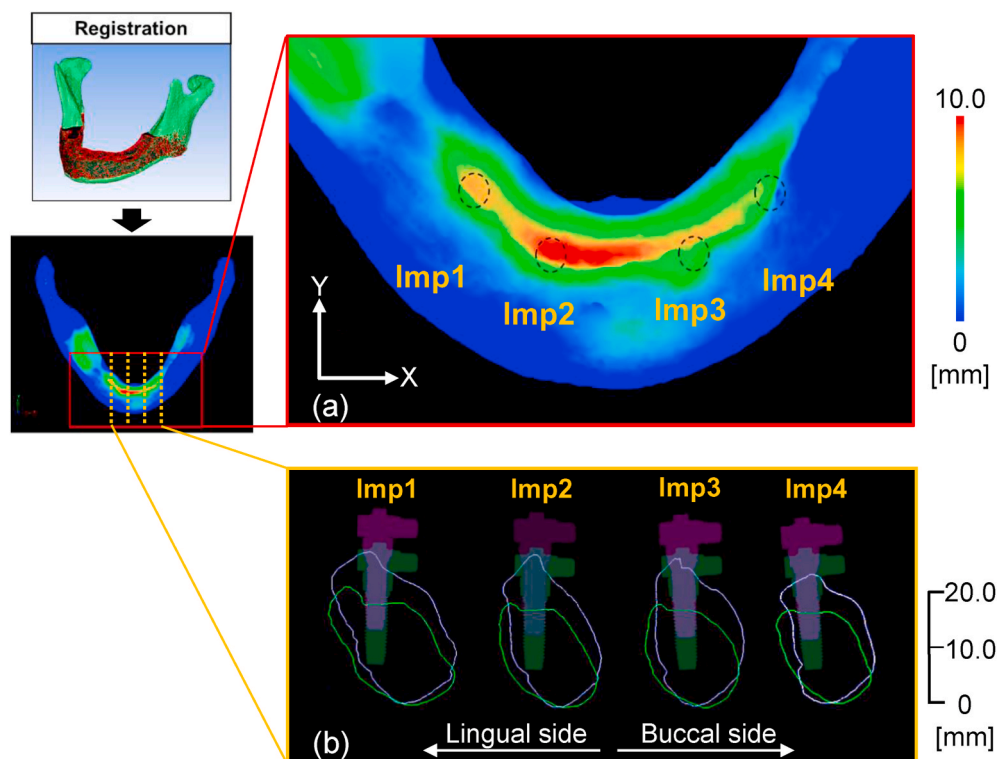


Fig. 10. The morphological assessment of mandibular bone shape between two time points. (a) Contour map shows vertical dimensional changes between model-A and B. The positions of each implant were indicated by dotted circles. (b) The vertical dimensional changes in sagittal cross section through the center of each implants. The bone shape and implant positions in cross section (purple for Model A, green for Model B) were indicated.

According to previous retrospective cohort studies, the amount of bone loss in marginal bone around the implants was approximately 2 mm or more per decade [46]. The amount of marginal bone resorption was dependent upon the types of implant design and supra-structure [47]. Clinically, marginal bone loss commonly refers to the bone resorption around implant fixtures as shown in those reports. Besides, in the present subject, vertical bone height was significantly changed (Fig. 10) but marginal bone loss around the implants was slightly observed. In fact, the condition of the soft tissue has been stable for 12 years and implant thread was not exposed during the maintenance period. Therefore, the current implant positions are the result of a combination of peri-implant bone loss and changes in relative position to the mandible. Despite the lack of accurate measurements of the bone

loss surrounding the implants, Fig. 10 demonstrates significant changes in the shape of the mandibular bone after 12 years, approximately 9 mm surrounding Imp2. Despite the possible effect of the flattening of bones during the implant surgery and the immediate healing process following implantation [48], the changes of the bone are attributed to metabolic function and a mechanobiological reaction [36], which is clinically meaningful and should be considered. However, it is necessary to consider the validity of the references for the geometrical registration of the two models. In this study, the corner points on the mandibular angle and spina mentalis were used (Fig. 5). Since these anatomical points are insertions and origins of craniomandibular muscles, they should be appropriate as reference points. Due to the absence of control patient or control population in this study, it is unclear which physiological,

biological and mechano-biological factor is potentially associated with the bone remodeling phenomenon in this subject.

In this study, the subject wore a bar-clip attachment overdenture, which was supported by the implants and mucosa during oral function. Both components convey load to the bone. Suenaga et al. reported that denture base pressure affected bone metabolism based on the results of nuclear medicine scanning [49]. The morphological study of mandibular bone resorptions with implant overdentures reported that the average reduction in height was almost 1.0 mm in 5 years, and the bone height of the left posterior residual ridge was reduced by approximately 2 mm over a period of 12 years [50]. Considering the amount of bone reduction observed in their studies, chronological changes of the alveolar ridge shape were considered to be valid in the present study. Our study simulated the loads on the implants, showing the biomechanical behaviors of the bone surrounding the implants to be reasonable. On the other hand, the relationship between the biomechanical behavior of the posterior residual ridge and the morphological changes in the mandibular bone, especially in the mucosa beneath the denture, were not demonstrated in this study, because the denture base and mucosa were not constructed in the FE models, and the biomechanical behavior in the mucosa beneath the denture is presumably different from that of the clinical condition.

This study has some limitations. Even though the CT data for model B were reconstructed with the SEMAR algorithm to minimize the beam hardening, it could not be completely avoided. Thus, manual segmentation was needed during the FE modeling process. Also, it is well known that the use of a reference phantom leads to more credible calibration between HU and BMD in CT-FEA studies [51]. On the model side, even though the model represented the heterogeneous bone material properties from HU, we should pay attention to uncertainties in the trabecular bone that could affect the computed values in FEA [52,53]. In the present study, a part of the mandible was constrained, in order to clarify the mechanical state around each implant in both models. It should be noted that the musculoskeletal constraints could affect the deformation of the mandible [54,55]. Despite the use of biological-data taken from the subject, the absence of experimental measurement for the validation of analysis results cannot be disregarded [56].

This study revealed that the mandibular bone had significantly changed by comparing the bone shape, qualities and quantities before and 12 years after implantation. As a result, the stress and strain distributions in the peri-implant bone were confirmed to be partially averaged. The results of this study elucidated the effectiveness of personalized FEA based on chronological changes in the shape of the bone and suggested that a living body adjusts itself to mechanical loads by bone remodeling surrounding implants.

5. Conclusion

From the comparison of FE models constructed from CT data obtained before and 12 years after-implantation, averaged intraosseous stress and strain were observed in Aged-model due to temporal changes in the mass and quality of the bone. The results suggesting that the mandibular bone is adapting to mechanical loads by bone remodeling.

Funding

This work was supported by JSPS KAKENHI Grant Numbers JP20K10047.

CRedit authorship contribution statement

Emika Sato: Methodology, Software, Writing - original draft. **Ryuji Shigemitsu:** Conceptualization, Methodology, Investigation, Writing - review & editing, Resources. **Takehiko Mito:** Formal analysis. **Nobuhiro Yoda:** Data curation. **John Rasmussen:** Data Processing, Visualization, Supervision, Writing - review & editing. **Keiichi Sasaki:**

Supervision, Writing - review & editing.

Declaration of competing interest

None declared.

Acknowledgements

The authors are grateful to Dr. Tetsuo Kawata for data collection and Dr. Hiroaki Takahashi for assisting in analyzing the data.

Appendix A. Supplementary data

Supplementary data to this article can be found online at <https://doi.org/10.1016/j.compbmed.2020.104173>.

References

- [1] J. Derks, D. Schaller, J. Hakansson, J.L. Wennstrom, C. Tomasi, T. Berglundh, Effectiveness of implant therapy analyzed in a Swedish population: prevalence of peri-implantitis, *J. Dent. Res.* 95 (2016) 43–49, <https://doi.org/10.1177/0022034515608832>.
- [2] C.E. Misch, M.L. Perel, H.L. Wang, G. Sammartino, P. Galindo-Moreno, P. Trisi, M. Steigmann, A. Rebaudi, A. Palti, M.A. Pikos, D. Schwartz-Arad, J. Choukroun, J. L. Gutierrez-Perez, G. Marenzi, D.K. Valavanis, Implant success, survival, and failure: the international congress of oral implantologists (ICOI) pisa consensus conference, *Implant Dent.* 17 (2008) 5–15, <https://doi.org/10.1097/ID.0b013e3181676059>.
- [3] C.J. Goodacre, G. Bernal, K. Rungcharassaeng, J.Y. Kan, Clinical complications in fixed prosthodontics, *J. Prosthet. Dent.* 90 (2003) 31–41, [https://doi.org/10.1016/S0022-3913\(03\)00214-2](https://doi.org/10.1016/S0022-3913(03)00214-2).
- [4] M. Aglietta, V.I. Siciliano, M. Zwahlen, U. Bragger, B.E. Pjetursson, N.P. Lang, G. E. Salvi, A systematic review of the survival and complication rates of implant supported fixed dental prostheses with cantilever extensions after an observation period of at least 5 years, *Clin. Oral Implants Res.* 20 (2009) 441–451, <https://doi.org/10.1111/j.1600-0501.2009.01706.x>.
- [5] C.J. Goodacre, G. Bernal, K. Rungcharassaeng, J.Y. Kan, Clinical complications with implants and implant prostheses, *J. Prosthet. Dent.* 90 (2003) 121–132, [https://doi.org/10.1016/S0022-3913\(03\)00212-9](https://doi.org/10.1016/S0022-3913(03)00212-9).
- [6] A.G. Robling, A.B. Castillo, C.H. Turner, Biomechanical and molecular regulation of bone remodeling, *Annu. Rev. Biomed. Eng.* 8 (2006) 455–498, <https://doi.org/10.1146/annurev.bioeng.8.061505.095721>.
- [7] H.M. Frost, Bone's mechanostat: a 2003 update, the anatomical record, Part A, Discoveries in molecular, cellular, and evolutionary biology 275 (2003) 1081–1101, <https://doi.org/10.1002/ar.a.10119>.
- [8] J.R. Kelly, P. Benetti, P. Rungruangnunt, A.D. Bona, The slippery slope: critical perspectives on in vitro research methodologies, *Dent. Mater.* 28 (2012) 41–51, <https://doi.org/10.1016/j.dental.2011.09.001>.
- [9] R. Coray, M. Zeltner, M. Özcan, Fracture strength of implant abutments after fatigue testing: a systematic review and a meta-analysis, *J. Mech. Behav. Biomed. Mater.* 62 (2016) 333–346, <https://doi.org/10.1016/j.jmbbm.2016.05.011>.
- [10] E.A. Bonfante, P.G. Coelho, A critical perspective on mechanical testing of implants and prostheses, *Adv. Dent. Res.* 28 (2016) 18–27, <https://doi.org/10.1177/0022034515624445>.
- [11] T. Brosh, R. Pilo, D. Sudai, The influence of abutment angulation on strains and stresses along the implant/bone interface: comparison between two experimental techniques, *J. Prosthet. Dent.* 79 (1998) 328–334, [https://doi.org/10.1016/S0022-3913\(98\)70246-X](https://doi.org/10.1016/S0022-3913(98)70246-X).
- [12] Y. Matsudate, N. Yoda, M. Nanba, T. Ogawa, K. Sasaki, Load distribution on abutment tooth, implant and residual ridge with distal-extension implant-supported removable partial denture, *J. Prosthodont. Res.* 60 (2016) 282–288, <https://doi.org/10.1016/j.jpor.2016.01.008>.
- [13] J.P.M. Tribst, A.M.O. Dal Piva, M.A. Bottino, R.S. Nishioka, A.L.S. Borges, M. Özcan, Digital image correlation and finite element analysis of bone strain generated by implant-retained cantilever fixed prosthesis, *Eur. J. Prosthodont. Restor. Dent.* 28 (2020) 10–17, <https://doi.org/10.1922/EJPRD.1941Tribst08>.
- [14] A.A. Pesqueira, M.C. Goiato, H.G. Filho, D.R. Monteiro, D.M. Santos, M.F. Haddad, E.P. Pellizzer, Use of stress analysis methods to evaluate the biomechanics of oral rehabilitation with implants, *J. Oral Implantol.* 40 (2014) 217–228, <https://doi.org/10.1563/AID-JOI-D-11-00066>.
- [15] K. Kubo, T. Kawata, H. Suenaga, N. Yoda, R. Shigemitsu, T. Ogawa, K. Sasaki, Development of in vivo measuring system of the pressure distribution under the denture base of removable partial denture, *J. Prosthodont. Res.* 53 (2009) 15–21, <https://doi.org/10.1016/j.jpor.2008.08.006>.
- [16] H. Suenaga, K. Kubo, R. Hosokawa, T. Kuriyagawa, K. Sasaki, Effects of occlusal rest design on pressure distribution beneath the denture base of a distal extension removable partial denture-an in vivo study, *Int. J. Prosthodont.* 27 (2014) 469–471, <https://doi.org/10.11607/ijp.3847>.
- [17] M.S. Reddy, R. Sundram, H.A. Eid Abdemagdy, Application of finite element model in implant dentistry: a systematic review, *J. Pharm. BioAllied Sci.* 11 (2019) 85–91, https://doi.org/10.4103/JPBS.JPBS_296_18.

- [18] Y.C. Cheng, D.H. Lin, C.P. Jiang, S.Y. Lee, Design improvement and dynamic finite element analysis of novel ITI dental implant under dynamic chewing loads, *Bio Med. Mater. Eng.* 26 (Suppl 1) (2015) 555–561, <https://doi.org/10.3233/BME-151346>.
- [19] Y. Matsuura, H. Giambini, Y. Ogawa, Z. Fang, A.R. Thoreson, M.J. Yaszemski, L. Lu, An Specimen-specific nonlinear finite element modeling to predict vertebrae fracture loads after vertebroplasty, *Spine (Phila Pa 39)* (1976) 1291–1296, <https://doi.org/10.1097/BRS.0000000000000540>, 2014.
- [20] R. Shigemitsu, T. Ogawa, T. Matsumoto, N. Yoda, Y. Gunji, Y. Yamakawa, K. Ikeda, K. Sasaki, Stress distribution in the peri-implant bone with splinted and non-splinted implants by in vivo loading data-based finite element analysis, *Odontology* 101 (2013) 222–226, <https://doi.org/10.1007/s10266-012-0077-y>.
- [21] N. Wakabayashi, M. Ona, T. Suzuki, Y. Igarashi, Nonlinear finite element analyses: advances and challenges in dental applications, *J. Dent.* 18 (Suppl 3) (2007) 463–471, <https://doi.org/10.1016/j.jdent.2008.03.010>.
- [22] P. Streckbein, R.G. Streckbein, J.F. Wilbrand, C.Y. Malik, H. Schaaf, H.P. Howaldt, M. Flach, Non-linear 3D evaluation of different oral implant-abutment connections, *J. Dent. Res.* 91 (2012) 1184–1189, <https://doi.org/10.1177/0022034512463396>.
- [23] M. Wada, T. Andoh, T. Gonda, Y. Maeda, Implant placement with a guided surgery system based on stress analyses utilizing the bone density: a clinical case report, *J. Oral Implantol.* 40 (2014) 603–606, <https://doi.org/10.1563/AAID-JOI-D-12-00194>.
- [24] N. Yoda, K. Zheng, J. Chen, W. Li, M. Swain, K. Sasaki, Q. Li, Bone morphological effects on post-implantation remodeling of maxillary anterior buccal bone: a clinical and biomechanical study, *J. Prosthodont. Res.* 61 (2017) 393–402, <https://doi.org/10.1016/j.jpor.2016.12.010>.
- [25] T. Kawata, N. Yoda, T. Kawaguchi, T. Kuriyagawa, K. Sasaki, Behaviours of three-dimensional compressive and tensile forces exerted on a tooth during function, *J. Oral Rehabil.* 34 (2007) 259–266, <https://doi.org/10.1111/j.1365-2842.2007.01681.x>.
- [26] N. Yoda, T. Ogawa, Y. Gunji, J.R. Vanegas, T. Kawata, K. Sasaki, Effects of food texture on three-dimensional loads on implants during mastication based on in vivo measurements, *Implant Dent.* 25 (2016) 515–519, <https://doi.org/10.1097/ID.0000000000000443>.
- [27] R. Shigemitsu, N. Yoda, T. Ogawa, T. Kawata, Y. Gunji, Y. Yamakawa, K. Ikeda, K. Sasaki, Biological-data-based finite-element stress analysis of mandibular bone with implant-supported overdenture, *Comput. Biol. Med.* 54c (2014) 44–52, <https://doi.org/10.1016/j.combiomed.2014.08.018>.
- [28] P.A.G. Teixeira, J.-B. Meyer, C. Baumann, A. Raymond, F. Sirveaux, H. Coudane, A. Blum, Total hip prosthesis CT with single-energy projection-based metallic artifact reduction: impact on the visualization of specific periprosthetic soft tissue structures, *Skeletal Radiol.* 43 (2014) 1237–1246, <https://doi.org/10.1007/s00256-014-1923-5>.
- [29] K. Yasaka, E. Maeda, S. Hanaoka, M. Katsura, J. Sato, K. Ohtomo, Single-energy metal artifact reduction for helical computed tomography of the pelvis in patients with metal hip prostheses, *Jpn. J. Radiol.* 34 (2016) 625–632, <https://doi.org/10.1007/s11604-016-0566-y>.
- [30] M. Dalstra, R. Huiskes, L. van Erning, Development and validation of a three-dimensional finite element model of the pelvic bone, *J. Biomech. Eng.* 117 (1995) 272–278, <https://doi.org/10.1115/1.2794181>.
- [31] D. Tawara, J. Sakamoto, J. Oda, Finite element analysis considering material inhomogeneity of bone using “ADVENTURE System”, in: *JSME International Journal Series C Mechanical Systems, Machine Elements and Manufacturing* 48, 2005, pp. 292–298.
- [32] K. Watanabe, H. Mutsuzaki, T. Fukaya, T. Aoyama, S. Nakajima, N. Sekine, K. Mori, Development of a Knee Joint CT-FEM Model in Load Response of the Stance Phase during Walking Using Muscle Exertion, Motion Analysis, and Ground Reaction Force Data, Kaunas), *Medicina*, 2020, p. 56.
- [33] J.H. Keyak, S.A. Rossi, K.A. Jones, H.B. Skinner, Prediction of femoral fracture load using automated finite element modeling, *J. Biomech.* 31 (1998) 125–133, [https://doi.org/10.1016/s0021-9290\(97\)00123-1](https://doi.org/10.1016/s0021-9290(97)00123-1).
- [34] R. Huiskes, Adaptive bone-remodeling theory applied to prosthetic-design analysis, *J. Biomech.* 20 (1987) 1135–1150, [https://doi.org/10.1016/0021-9290\(87\)90030-3](https://doi.org/10.1016/0021-9290(87)90030-3).
- [35] D. Lin, Q. Li, W. Li, N. Duckmanton, M. Swain, Mandibular bone remodeling induced by dental implant, *J. Biomech.* 43 (2010) 287–293, <https://doi.org/10.1016/j.jbiomech.2009.08.024>.
- [36] D.J. Hadjidakis, I.I. Androulakis, Bone remodeling, *Ann. N. Y. Acad. Sci.* 1092 (2006) 385–396, <https://doi.org/10.1196/annals.1365.035>.
- [37] J.P. Geng, K.B. Tan, G.R. Liu, Application of finite element analysis in implant dentistry: a review of the literature, *J. Prosthet. Dent* 85 (2001) 585–598, <https://doi.org/10.1067/mp.2001.115251>.
- [38] M.N. Castro, J. Rasmussen, S. Bai, M.S. Andersen, Validation of subject-specific musculoskeletal models using the anatomical reachable 3-D workspace, *J. Biomech.* 90 (2019) 92–102, <https://doi.org/10.1016/j.jbiomech.2019.04.037>.
- [39] T.W. Koriath, A. Versluis, Modeling the mechanical behavior of the jaws and their related structures by finite element (FE) analysis, *Critical reviews in oral biology and medicine* 8 (1997) 90–104, <https://doi.org/10.1177/10454411970080010501>.
- [40] A.H. Burstein, J. Zika, K. Heiple, L. Klein, Contribution of collagen and mineral to the elastic-plastic properties of bone, *JBS* 57 (1975) 956–961.
- [41] H. Peterlik, P. Roschger, K. Klaushofer, P. Fratzl, From brittle to ductile fracture of bone, *Nat. Mater.* 5 (2006) 52, <https://doi.org/10.1038/nmat1545>.
- [42] H. Weinans, R. Huiskes, H. Grootenboer, Effects of fit and bonding characteristics of femoral stems on adaptive bone remodeling, *J Biomech Eng.* 116 (1994) 393–400, <https://doi.org/10.1115/1.2895789>.
- [43] R. Huiskes, If bone is the answer, then what is the question? *J. Anat.* 197 (Pt 2) (2000) 145–156, <https://doi.org/10.1046/j.1469-7580.2000.19720145.x>.
- [44] S. Inoue, M. Kawara, T. Iida, M. Iwasaki, O. Komiyama, T. Kaneda, Analysis of correlation between height of residual ridge and bone density of residual ridge crest at edentulous mandible using computed tomography, *J. Prosthodont. Res.* 61 (2017) 371–378, <https://doi.org/10.1016/j.jpor.2016.09.003>.
- [45] J. Wolff, *Das Gesetz der Transformation der Knochen*, 1892.
- [46] D. French, D.L. Cochran, R. Ofec, Retrospective cohort study of 4,591 strumann implants placed in 2,060 patients in private practice with up to 10-year follow-up: the relationship between crestal bone level and soft tissue condition, *Int. J. Oral Maxillofac. Implants* 31 (2016) 168–178, <https://doi.org/10.11607/jomi.4932>.
- [47] S.Y. Lee, J.Y. Koak, S.K. Kim, I.C. Rhyu, Y. Ku, S.J. Heo, C.H. Han, A long-term prospective evaluation of marginal bone level change around different implant systems, *Int. J. Oral Maxillofac. Implants* 31 (2016) 657–664, <https://doi.org/10.11607/jomi.3932>.
- [48] M. Hudieb, S. Kasugai, Biomechanical effect of crestal bone osteoplasty before implant placement: a three-dimensional finite element analysis, *Int. J. Oral Maxillofac. Surg.* 40 (2011) 200–206, <https://doi.org/10.1016/j.ijom.2010.10.002>.
- [49] H. Suenaga, J. Chen, K. Yamaguchi, W. Li, K. Sasaki, M. Swain, Q. Li, Mechanobiological bone reaction quantified by positron emission tomography, *J. Dent. Res.* 94 (2015), <https://doi.org/10.1177/0022034515573271>, 738–734.
- [50] K. Kordatzis, P.S. Wright, H.J. Meijer, Posterior mandibular residual ridge resorption in patients with conventional dentures and implant overdentures, *Int. J. Oral Maxillofac. Implants* 18 (2003) 447–452.
- [51] P. Mah, T.E. Reeves, W.D. McDavid, Deriving Hounsfield units using grey levels in cone beam computed tomography, *Dentomaxillofacial Radiol.* 39 (2010) 323–335, <https://doi.org/10.1259/dmfr/31640433>.
- [52] J. Du, J.H. Lee, A.T. Jang, A. Gu, M. Hossaini-Zadeh, R. Prevost, D.A. Curtis, S. P. Ho, Biomechanics and strain mapping in bone as related to immediately-loaded dental implants, *J. Biomech.* 48 (2015) 3486–3494, <https://doi.org/10.1016/j.jbiomech.2015.05.014>.
- [53] Q.Y. Mao, K.N. Su, Y.X. Zhou, M. Hossaini-Zadeh, G.S. Lewis, J. Du, Voxel-based micro-finite element analysis of dental implants in a human cadaveric mandible: tissue modulus assignment and sensitivity analyses, *Journal of the Mechanical Behavior of Biomedical Materials* 94 (2019) 229–237, <https://doi.org/10.1016/j.jmbm.2019.03.008>.
- [54] T.W. Koriath, A.G. Hannam, Mandibular forces during simulated tooth clenching, *J. Orofac. Pain* 88 (1992) 178–189.
- [55] R. Shigemitsu, K. Sasaki, J. Rasmussen, Musculoskeletal modeling with jaw motion data from a TMD patient, *Advances in Transdisciplinary Engineering* 11 (2020) 108–114, <https://doi.org/10.3233/ATDE200015>.
- [56] Y. Chang, A. Tambe, Y. Maeda, T. Gonda, Finite element analysis of dental implants with validation: to what extent can we expect the model to predict biological phenomena? A literature review and proposal for classification of a validation process, *Int J Implant Dent* 4 (2018) 7.